11-3-2008

Coherent control of nanomagnet dynamics via ultrafast spin torque pulses

Samir Garzon
University of South Carolina - Columbia

Longfei Ye
University of South Carolina - Columbia

Richard A. Webb
University of South Carolina - Columbia, webbra@mailbox.sc.edu

Thomas M. Crawford
University of South Carolina - Columbia

Mark Covington

See next page for additional authors

Publication Info

Published in *Physical Review B*, Volume 78, Issue 18, 2008, pages 180401-1-180401-4.
Garzon, S., Longfei, Y., Webb, R.A., Crawford, T.M., Covington, M., and Kaka, S. (2008). Coherent control of nanomagnet dynamics via ultrafast spin torque pulses. *Physical Review B, 78*(18), 180401-1 - 180401-4. doi: 10.1103/PhysRevB.78.180401

Selected for a Viewpoint in *Physics*

RAPID COMMUNICATIONS

PHYSICAL REVIEW B **78**, 180401(R) (2008)

Coherent control of nanomagnet dynamics via ultrafast spin torque pulses

Samir Garzon,[1] Longfei Ye,[1] Richard A. Webb,[1] Thomas M. Crawford,[1] Mark Covington,[2] and Shehzaad Kaka[2]

[1]*Physics and Astronomy Department and USC Nanocenter, University of South Carolina, Columbia, South Carolina 29208, USA*

[2]*Seagate Research, 1251 Waterfront Place, Pittsburgh, Pennsylvania 15222, USA*

(Received 22 July 2008; revised manuscript received 2 September 2008; published 3 November 2008)

We demonstrate reliable manipulation of the magnetization dynamics of a precessing nanomagnet by precisely controlling the spin transfer torque on the subnanosecond time scale. Using a simple pulse shaping scheme consisting of two ultrafast spin torque pulses with variable amplitudes and delay, we demonstrate coherent control over the precessional orbits and the ability to tune the switching probability of a nanomagnet at room temperature and 77 K. Our measurements suggest that appropriately shaped spin transfer can be used to efficiently manipulate the orientation of a free layer nanomagnet, thus providing an alternative for spin torque driven spintronic devices.

DOI: 10.1103/PhysRevB.78.180401 PACS number(s): 75.75.+a, 72.25.Ba, 73.63.−b

The magnetization orientation of a nanoscale ferromagnet can be manipulated using an electric current via the spin transfer effect:[1–4] spin angular momentum is transferred from the conduction to the localized electrons, exerting an effective torque on the ferromagnet.[5–8] Time domain measurements of nanopillar devices at low temperatures have directly shown that magnetization dynamics and reversal occur coherently over a time scale of nanoseconds.[9,10] By adjusting the shape of a spin torque wave form over a time scale comparable to the free precession period, control of the magnetization dynamics in nanopillar devices should be possible.[11–13] Here we report coherent control of the free layer magnetization in nanopillar devices using a pair of current pulses as narrow as 30 ps with adjustable amplitudes and delay. In contrast with previous measurements where the spin torque is applied throughout a large fraction of a precession cycle,[14–18] in our experiments the magnetization evolves freely except for short time intervals when it is driven by the spin torque. By using ultrashort spin torque "impulses," we can access a previously unexplored regime in which nanomagnet dynamics is strongly affected by the timing of the spin torque pulses with respect to the underlying free precession orbits. We experimentally map the regions where the spin torque "impulses" have the largest effect on the dynamics, thus increasing the efficiency of nanomagnet switching over longer spin torque pulses. Furthermore, we can manipulate the free magnetic moment motion, exciting large-angle precession and demonstrating room-temperature coherent dynamics.

We first discuss measurements of type "N" $Co_{90}Fe_{10}$(8.7 nm)/Cu(3 nm)/$Co_{90}Fe_{10}$(2 nm) spin transfer nanopillar devices, which are patterned into ~150 $\times 75$ nm^2 ellipses as shown in Fig. 1(a). Antiferromagnetic dipolar field coupling between the thick layer (polarizer) and the "free" layer is canceled by biasing the devices with an easy-axis magnetic field $H_{\parallel} \sim 800$ Oe [Fig. 1(b)]. The free layer can be switched between low resistance (parallel, P) and high resistance (antiparallel, AP) states via a spin transfer torque from an applied dc current [Fig. 1(c)] with polarity defined in Fig. 1(a). Typical values of the four terminal P state resistance and of the magnetoresistance are 1.3 Ω and 9%, respectively. The large resistance values shown in Figs. 1(b) and 1(c) are due to lead resistance together with inductive impedance in the experimental setup. Using a femtosecond mode-locked laser in single-shot mode, we generate either a single optical pulse or a pair of optical pulses with adjustable amplitudes and time delay t_D, which are then converted to electrical pulses using a LT-GaAs/Au photoconductive switch.[19,20] Our optically generated electrical pulses can be relatively timed with subpicosecond resolution, and since our measurement is independent of the absolute pulse timing, there are no trigger jitter effects. Reflection measurements show that typical room-temperature pulse widths at the device are ~30 ps, but due to cryostat bandwidth limitations the typical pulse widths are ~58 ps at 77 K. In our devices the small-angle free precession period $\tau \sim 300$ ps (calculated from thin-film measurements of M_S and the nominal shape anisotropy) is much larger than the current pulse width τ_ω but comparable to the interpulse delay $0 < t_D < 2$ ns. A 40-GHz bias tee is used to inject both the current pulses that induce magnetization dynamics and the ac/dc currents used to measure the resistance and reset the device. For each switching attempt, (i) the device is reset to the P state by applying a negative ~300 ms current step, (ii) the device state is confirmed by measuring the resistance, (iii) a simple shaped wave form, consisting of either one or two current pulses, is used to induce nanomagnet dynamics, and (iv) the final state of the multilayer is probed by measuring its steady-state resistance. For all reported measurements the number of repetitions is chosen to ensure that the statistical error is smaller than 2%. It is known that at nonzero temperatures thermal excitations broaden the distribution of orientations of the free layer magnetization ($\vec{M}$) around the equilibrium direction. However, reproducibility in nanomagnet switching can be increased by applying transverse fields[17] or through interlayer coupling.[9] Throughout our measurements we apply in-plane transverse fields $H_{\perp} \sim 175$ Oe to shift the P and AP fixed points of $\vec{M}$ away from the easy axis [Fig. 1(a)] to obtain a nonzero equilibrium angle between the polarizer and free layer (noncollinear geometry).

We first demonstrate ~100% switching probability (P_S) with single 30 ps pulses at room temperature [Fig. 1(d)]. In particular, for devices with dc switching currents comparable to those previously reported[15,16] we achieve $P_S \approx 100\%$ with

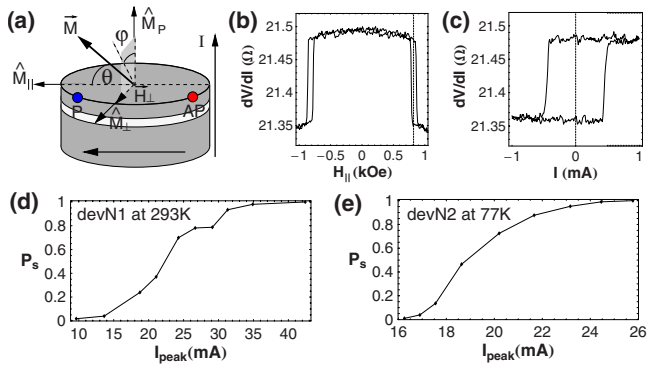

FIG. 1. (Color online) (a) Schematic of a type N nanopillar. Unit vectors $\hat{M}_{||}$, $\hat{M}_{\perp}$, and $\hat{M}_P$ along the easy axis, in-plane hard axis, and out-of-plane direction, respectively, are shown. The orientation of $\vec{M}$ is defined by the polar angle θ measured from $\hat{M}_{||}$ and the azimuthal angle φ between $\hat{M}_P$ and the projection of $\vec{M}$ onto the $\hat{M}_P$-$\hat{M}_{\perp}$ plane. A transverse applied field $H_{\perp}$ shifts the P and AP energy minima away from $\hat{M}_{||}$. [(b) and (c)] Differential resistance vs (b) easy axis field and (c) current for device N2 at room temperature. In (c), $H_{||}$=830 Oe and $H_{\perp}$=175 Oe. [(d) and (e)] P_S vs single-pulse amplitude for devices (d) N1 at room temperature and (e) N2 at 77 K. Pulse durations are (d) ~30 ps and (e) ~58 ps full width at half maximum (FWHM).

pulse amplitudes two times smaller than expected from the assumption of pulse width and amplitude being inversely proportional.[21,22] These results are supported by macrospin simulations, which indicate that for the noncollinear geometry the pulse width–current product required for P_S=95% decreases by more than a factor of 2 when $\tau_w \ll \tau$. The reduction in pulse amplitude occurs because the effect of spin torque produced by longer pulses over a precession cycle is partially canceled. Depending on field bias, temperature, and device anisotropy, P_S shows either a stepped [note feature at $P_S \approx 0.8$ in Fig. 1(d)] or smooth [Fig. 1(e)][15,16] monotonic increase with increasing pulse amplitude. The stepped increase in P_S, predicted by our simulations and previously observed in similar experiments as a function of pulse width ($\tau_\omega > 100$ ps),[17] is due to the underlying free precession orbits.

In order to explore the coherence of nanomagnet evolution, we use an ultrashort pulse to excite the magnetization dynamics and apply a second ultrashort pulse of equal amplitude at different instants of the free precession orbit. The switching probability of device N2 as a function of interpulse delay at room temperature and 77 K is shown in Figs. 2(a) and 2(b). Since incoherent dynamics would lead to a delay-independent switching probability $P_2 = 1-(1-P_1)^2$ (where P_1 is the single-pulse switching probability), our data indicate that coherent nanomagnet dynamics occurs even at room temperature. However, we observe a striking difference between the slow change in P_S at room temperature and the clear oscillations and strong modulation present at 77 K. The devices described so far (type N), with dc switching currents ~0.4 mA, have a small stability factor $\Delta = E_B/k_BT$ (where E_B is the P-AP energy barrier), and thus are extremely sensitive to thermal effects. At room temperature, the probability

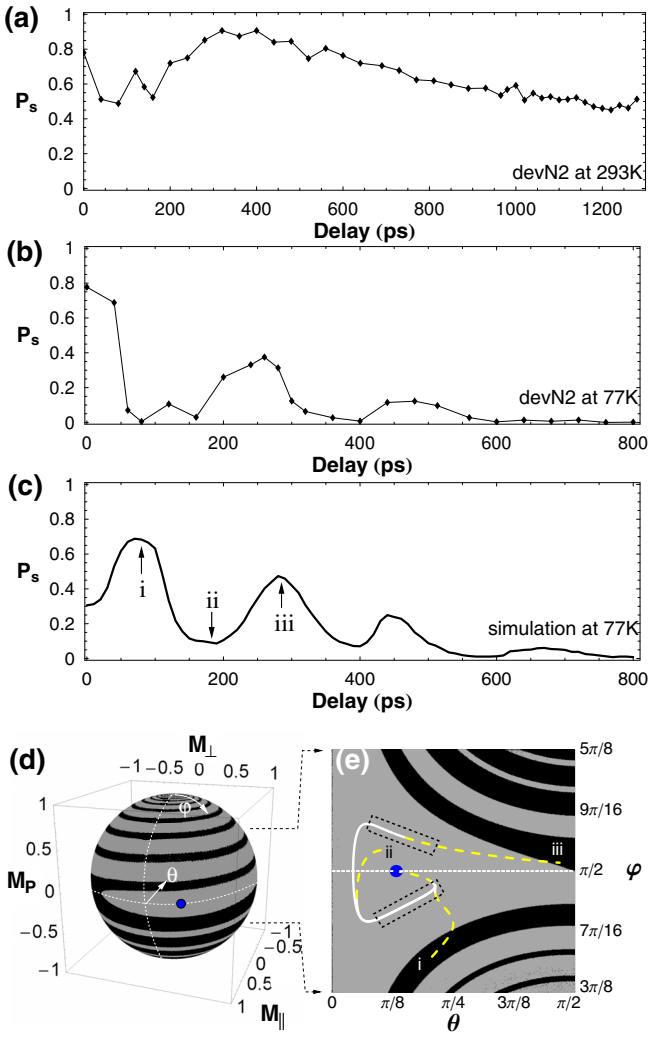

FIG. 2. (Color online) P_S of device N2 at (a) 293 and (b) 77 K as a function of delay between two current pulses. (c) Simulated P_S vs delay for two equal amplitude 58 ps FWHM pulses at 77 K. Labeled regions correspond to the orbits shown in (e). (d) Phase portrait of $\vec{M}$ showing the basins of attraction for the two stable points P and AP. (Stable point AP is not visible in the figure.) The angles and axes are defined in Fig. 1(a). Initial conditions θ_0 and φ_0 within the gray (black) basin lead to no switching (switching). (e) $\vec{M}$ trajectories generated by two current pulses of equal amplitude that have been delayed by 90 (i), 190 (ii), and 280 ps (iii). Yellow (dashed) lines show the response of $\vec{M}$ to spin torque pulses, while white (solid) lines show free evolution. Rectangles enclose regions where a second pulse has high probability of switching $\vec{M}$.

of thermally assisted switching increases and the distribution of the initial orientations is much broader. While thermally assisted switching only increases the baseline of P_S, the broadening of the distribution of initial orientations decreases the reproducibility of the trajectories at each repetition of the experiment, partially averaging out the delay dependence. This averaging explains why at room temperature type N devices typically show decay in P_S with increasing delay and only small amplitude P_S oscillations.

To understand the origin of the oscillations, which are clearly observed at 77 K, we model the time evolution of the

magnetization of a single domain nanomagnet driven by a perpendicular spin current [Fig. 1(a)] by using a modified Landau-Lifshitz-Gilbert (LLG) equation, which includes the Slonczewski spin torque term with $g(\theta)=\text{const.}$[2,23] We assume that the magnetization of the polarizer is fixed and consider the effect of nonzero temperatures only on the distribution of initial orientations of $\vec{M}$ (via a Monte Carlo method) but not on the evolution of $\vec{M}$, which is assumed to be completely deterministic. Since $\vec{M}$ has constant magnitude M_S and is fully determined by the angles θ and φ defined in Fig. 1(a), it can be represented as a point in the unit sphere shown in Fig. 2(d). By coloring in black (gray) the initial magnetization directions (θ_0, φ_0) for which free evolution governed by the LLG equation leads to switching (no switching), the phase portrait of $\vec{M}$ in the absence of spin torque can be found.[24] The black and gray regions, which are the basins of attraction for the P and AP energy minima (located at $\varphi=\pi/2$, $\theta=\arcsin H_\perp/H_k$ and $\varphi=\pi/2$, $\theta=\pi-\arcsin H_\perp/H_k$, respectively, where H_k is the easy axis anisotropy field), are wrapped around each other, emphasizing the final state's large sensitivity to fluctuations in the initial orientation of $\vec{M}$ (i.e., thermal effects).

Simulations of the delay dependence of P_S for a pair of pulses with equal amplitude at 77 K [Fig. 2(c)] show oscillations with delay that agree qualitatively with our observations [Fig. 2(b)]. Typical trajectories at consecutive maxima and minima of P_S, regions labeled i, ii, and iii, in Fig. 2(c) are shown in Fig. 2(e), where the section with $0<\theta<\pi/2$ and $3\pi/8<\varphi<5\pi/8$ of the phase portrait shown in Fig. 2(d) has been stretched into a plane. The initial condition and first pulse (dashed yellow line) are equivalent for all trajectories, but the second pulse (dashed yellow line) is applied at different times (t_D=90, 190, and 280 ps). The free evolution between the two pulses is shown in white. We observe that there are two regions [dashed boxes in Fig. 2(e)] where the second spin torque pulse can more effectively induce basin boundary crossing and lead to magnetization reversal. As indicated by trajectory ii, a second pulse applied outside of the marked regions can even push $\vec{M}$ closer to the P fixed point, reducing the effect from the first pulse. These simulations illustrate how in the noncollinear geometry, when a pulse with a width larger than the free precession period is used for nanomagnet switching, partial cancellation of the effect of spin torque occurs, decreasing P_S.

To clearly demonstrate room-temperature coherent control, we have performed similar measurements on type "E" devices, which have switching currents ~2 mA and higher thermal stability. These devices have an extended bottom layer and are comprised of $[Ni_{80}Fe_{20}(20\ \text{nm})/Co_{90}Fe_{10}(2\ \text{nm})]/Cu(10\ \text{nm})/Co_{90}Fe_{10}(3\ \text{nm})$, where the extended bottom layer [NiFe/CoFe] decreases the magnetic layer dipolar coupling. Typical traces of P_S as a function of delay are shown in Figs. 3(a) and 3(b) at room temperature and 77 K. Clear large amplitude oscillations in P_S can be seen even at room temperature for up to 1 ns. Fourier analysis of the oscillations of device E1 (with nominal dimensions $150\times75\ \text{nm}^2$) at 77 K shows a fundamental period of 120 ps (ω=8.3 GHz) and a much smaller 2ω harmonic. Since

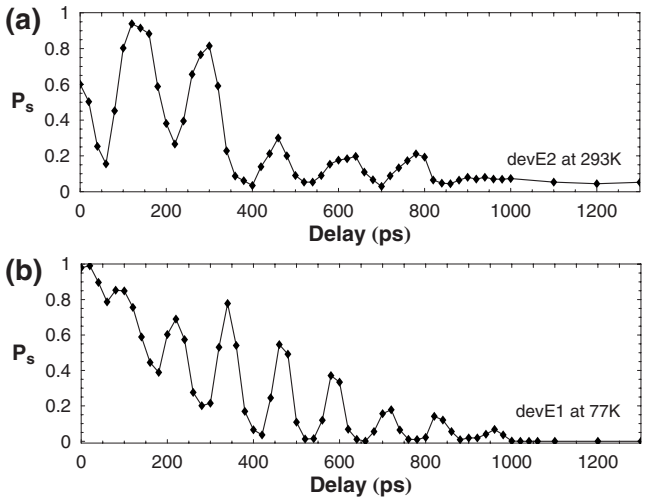

FIG. 3. P_S vs delay for extended bottom layer devices (a) E2 at room temperature and (b) E1 at 77 K.

the precession period is twice the period of the P_S oscillations, $\tau\approx240$ ps for device E1. Similarly, for device E2 with nominal dimensions $160\times100\ \text{nm}^2$, $\tau\approx330$ ps. The precession periods obtained in this way are consistent with estimations based on thin-film measurements of M_S and demagnetization coefficients of ellipsoidal nanomagnets with the dimensions given above. At room temperature the switching probability of device E2 can be tuned between 4% and 94% by only adjusting the delay between pulses. The enhancement in the switching probability from 60% at zero delay (single pulse) to ~94% at 120 ps delay [Fig. 3(a)] has been measured while keeping the amplitude of the pulses constant and thus the energy delivered to the device at zero delay is twice as large as that delivered by nonoverlapping pulses at longer delays. However, if instead the total energy delivered by the pulses is kept constant (data not shown), a more dramatic enhancement in P_S from 10% to 70% at intermediate pulse amplitudes and from 40% to 95% at larger pulse amplitudes is observed. Therefore, multiple current pulses timed with the underlying coherent dynamics require less total energy than a single pulse to reproducibly switch spin transfer devices.

Increased control over the magnetization trajectory can be obtained by adjusting not only the pulses' timing but also their amplitude. We measure the switching probability as a function of the amplitude of a pair of pulses while keeping the delay (185 ps) and relative amplitude ($I_1/I_2=1$) constant [Fig. 4(a)]. P_S initially increases with increasing pulse amplitude but after 15 mA it decreases from 80% to 55% before finally increasing to ~100% at 23 mA. This counterintuitive result that increasing the spin torque leads to a decrease in the switching probability is fully consistent with coherent precession and is predicted by our simulations [Fig. 4(b)]. This agreement shows once more that in our system the macrospin model captures the essence of nanomagnet dynamics. Typical magnetization trajectories at the three labeled regions of Fig. 4(b) are shown in Fig. 4(c). As the amplitude of the pair of pulses is increased from regions I to II [Fig. 4(b)], the state of $\vec{M}$ at the end of the second pulse moves from the

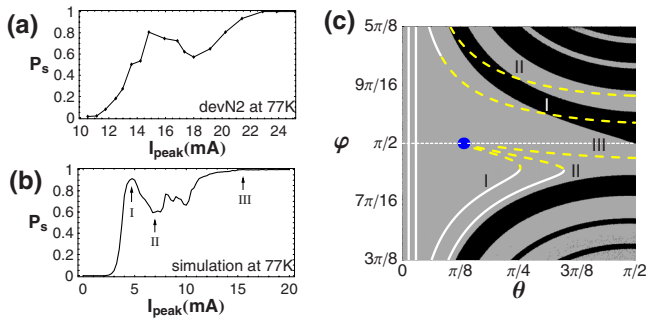

FIG. 4. (Color online) (a) P_S vs pulse pair amplitude at 185 ps delay and 77 K for device N2. (b) Simulated P_S for situation described in (a) using the same parameters as Fig. 2(b). (c) $\vec{M}$ trajectories at labeled regions of (b) corresponding to pulse amplitudes of 4.8 (I), 6.8 (II), and 15 mA (III). Initial conditions are chosen randomly with a thermal probability distribution. Yellow (dashed) and white (solid) lines are defined in caption to Fig. 2.

black basin to a higher-energy gray basin region, therefore decreasing P_S [Fig. 4(c)]. As the amplitude of the pulses is increased further to region III in Fig. 4(b), the first pulse produces enough spin torque to switch $\vec{M}$ [Fig. 4(c)]. These results suggest that by applying multiple short current pulses with controlled amplitudes and delays, the magnetization can be deliberately moved into higher-energy orbits.

In conclusion, we observe that single ~30 ps pulses switch noncollinear configuration devices using less total spin momentum transfer than longer (~1 ns) pulses. Furthermore, a pair of short pulses with appropriately adjusted amplitudes and relative timing can (i) increase the switching probability over its single-pulse value while requiring less energy and (ii) excite the magnetization into large-angle precession orbits. However, the distribution of initial orientations of $\vec{M}$ around its equilibrium direction limits both the switching efficiency and the probability of exciting large-angle orbits. Since this distribution depends on the temperature and the energy landscape around the magnetization equilibrium point, increased switching efficiency and ~100% probability of exciting large-angle precession require lower temperatures and higher stability of the energy minimum (which also lead to a higher precession frequency). As these conditions are satisfied, sharper modulation of P_S with pulse amplitude or delay will be observed. To achieve complete control over the magnetization (i.e., to set $\vec{M}$ into any desired orbit) requires not only a tight distribution of initial orientations of $\vec{M}$ but also multiple ultrashort pulses with precisely adjusted amplitudes and delays.

Our measurements also demonstrate coherence at room temperature and 77 K for up to 1 ns. Even though the decaying oscillations in the switching probability completely disappear above 1 ns, this does not imply lack of coherence as the decay arises mostly due to damping. Further measurements can help distinguish between damping and the long-time dephasing of trajectories corresponding to different repetitions of the experiment. Pulsed magnetization control can also be used to study the switching process in a variety of systems, including magnetic tunnel junctions, where a quiet "incubation" period that precedes magnetization switching has been observed.[18] Even though the required ultrashort pulses are not presently available in on-chip sources, our technique suggests an alternative, more efficient mechanism for resonantly pumping microwave oscillators[25,26] and for reversing magnetic memory bits in nanoscale magnetic random access memory (MRAM).

[1] J. C. Slonczewski, J. Magn. Magn. Mater. **159**, L1 (1996).
[2] J. C. Slonczewski, J. Magn. Magn. Mater. **195**, 261 (1999).
[3] L. Berger, Phys. Rev. B **54**, 9353 (1996).
[4] L. Berger, J. Appl. Phys. **49**, 2156 (1978).
[5] J. A. Katine, F. J. Albert, R. A. Buhrman, E. B. Myers, and D. C. Ralph, Phys. Rev. Lett. **84**, 3149 (2000).
[6] J. Z. Sun, J. Magn. Magn. Mater. **202**, 157 (1999).
[7] M. Tsoi, A. G. M. Jansen, J. Bass, W. C. Chiang, M. Seck, V. Tsoi, and P. Wyder, Phys. Rev. Lett. **80**, 4281 (1998).
[8] E. B. Myers *et al.*, Science **285**, 867 (1999).
[9] I. N. Krivorotov *et al.*, Science **307**, 228 (2005).
[10] Y. T. Cui, J. C. Sankey, C. Wang, K. V. Thadani, Z. P. Li, R. A. Buhrman, and D. C. Ralph, Phys. Rev. B **77**, 214440 (2008).
[11] K. Rivkin and J. B. Ketterson, Appl. Phys. Lett. **88**, 192515 (2006).
[12] L. Thomas *et al.*, Nature (London) **443**, 197 (2006).
[13] L. Thomas *et al.*, Science **315**, 1553 (2007).
[14] A. A. Tulapurkar *et al.*, Appl. Phys. Lett. **85**, 5358 (2004).
[15] S. Kaka *et al.*, J. Magn. Magn. Mater. **286**, 375 (2005).
[16] M. L. Schneider *et al.*, Appl. Phys. Lett. **90**, 092504 (2007).
[17] T. Devolder, C. Chappert, J. A. Katine, M. J. Carey, and K. Ito, Phys. Rev. B **75**, 064402 (2007).
[18] T. Devolder, J. Hayakawa, K. Ito, H. Takahashi, S. Ikeda, P. Crozat, N. Zerounian, J. V. Kim, C. Chappert, and H. Ohno, Phys. Rev. Lett. **100**, 057206 (2008).
[19] D. H. Auston, in *Picosecond Optoelectronic Devices*, edited by C. H. Lee (Academic, Orlando, 1984), pp. 73–117.
[20] F. W. Smith *et al.*, Appl. Phys. Lett. **54**, 890 (1989).
[21] R. H. Koch, J. A. Katine, and J. Z. Sun, Phys. Rev. Lett. **92**, 088302 (2004).
[22] Z. Li and S. Zhang, Phys. Rev. B **68**, 024404 (2003).
[23] J. Z. Sun, Phys. Rev. B **62**, 570 (2000).
[24] Y. B. Bazaliy, B. A. Jones, and S.-C. Zhang, Phys. Rev. B **69**, 094421 (2004).
[25] W. H. Rippard, M. R. Pufall, S. Kaka, S. E. Russek, and T. J. Silva, Phys. Rev. Lett. **92**, 027201 (2004).
[26] S. Kaka *et al.*, Nature (London) **437**, 389 (2005).